RESEARCH PAPER

PCCP
www.rsc.org/pccp

Quantum and classical equilibrium properties for exactly solvable models of weakly interacting systems

Serguei Patchkovskii* and Sergei N. Yurchenko

Contribution from the Steacie Institute for Molecular Sciences, NRC, 100 Sussex Drive, Ottawa, Ontario, Canada, K1A 0R6. E-mail: Serguei.Patchkovskii@nrc.ca

Received 26th April 2004, Accepted 4th June 2004
First published as an Advance Article on the web 18th June 2004

We investigate the importance of quantum-mechanical effects for equilibrium thermodynamics and the structure of weakly interacting systems. Two inclusion complexes with soft guest–host interaction potentials (endohedral ^{3}He buckminsterfullerene, ^{3}He@C_{60}, and H_2 molecule inside $(H_2O)_{20}$ cage) are examined by solving the Schrödinger equation for the nuclear motion of the guest. We demonstrate that quantum corrections are highly sensitive to the shape of the interaction potential. Anharmonic potential energy surfaces, exhibiting multiple, degenerate minima, magnify quantum contributions. Commonly used harmonic corrections are therefore unreliable for soft interaction potentials. We also show that quantum corrections to equilibrium constants and thermally averaged structural parameters may become significant at temperatures close to ambient. In the recently discovered hydrogen clathrate hydrate, quantum effects likely result in a $\sim$45 K decrease of the decomposition temperature at atmospheric pressure.

The importance of the quantization of nuclear motion for structure and properties is widely recognized in low-temperature and solid-state physics.[1,2] In physical chemistry, quantum effects are commonly implicated in dynamical processes, such as hydrogen transfer,[3] particularly in biological systems.[4] Dynamic behavior of some simple molecular systems under extreme conditions has also been demonstrated to be intrinsically quantum-mechanical.[5,6] In the calculations of thermodynamic properties of small rigid molecules, quantization of nuclear motion is usually taken into account in the harmonic approximation.[7] The more challenging and interesting case of molecular motion in soft anharmonic potentials is commonly treated with classical molecular dynamics simulations.[8] Large amplitudes of motion and small well depths, typical of soft potentials, make harmonic quantum corrections wildly inaccurate in such systems. Partly as a result, quantum contributions to equilibrium properties in such systems are tacitly assumed to be negligible.

An accurate description of molecular motion in soft potentials is particularly important for biological systems, where relatively small changes in equilibrium constants may lead to serious physiological consequences.[8] Another, technologically important, example is provided by hydrogen storage materials, where weak guest–host interactions are essential for ensuring the reversibility of the hydrogen adsorption process. The latter case is easily accessible for theoretical simulations, due to the simplicity of the interaction potentials.[9,10] In the recently discovered[11] hydrogen clathrates, the guest–host interaction potential is spherically symmetric to a good approximation.[9] In this case both classical and quantum equations of motion can be solved without introducing any additional approximations. This provides a simple, yet chemically meaningful test of quantum-mechanical effects for equilibrium thermodynamics and the structure of weakly interacting systems. In this work we compare quantum and classical statistics for two systems, where accurate *ab initio* interaction potentials are known.

Methods

We choose two model interaction potentials. Case A is the endohedral ^{3}He buckminsterfullerene, ^{3}He@C_{60}.[12,13] The MP2//TZP guest–host interaction in ^{3}He@C_{60} is given by (kcal mol^{-1}):[10]

$$v_A(r) = 0.6706r^6 + 0.5367r^4 + 1.370r^2 - 1.999 \qquad (1)$$

where r is the displacement from the cage center in ångström (Å). Potential v_A has a single soft minimum at the center of the cage. Case B is an H_2 molecule, inside the dodecahedral $(H_2O)_{20}$ cage (so called D-5^{12} cage[14,15]) of the type II hydrogen clathrate hydrate.[11] The MP2//DZP interaction potential in this case is given by:[9]

$$v_B(r) = 0.373r^6 - 0.140r^4 - 1.210r^2 - 1.84 \qquad (2)$$

where H_2 is assumed to be a structureless particle, and r is the displacement of the centre of the mass of the molecule from the cage centre, in Ångstroms.

This potential is bowler-hat-shaped, with the degenerate, spherical shell minimum $\approx$1.08 Å from the center of the cage. Potentials v_A and v_B are illustrated in Fig. 1. These two models are also important in their own right. The type II H_2/H_2O clathrate has the highest known extractable hydrogen/mass ratio, for any substance stable at the near-ambient conditions.[11] The endohedral fullerenes are important magnetic probes, with an incompletely understood formation mechanism.[16]

For both complexes the relevant equilibrium is described by the chemical reaction:

$$G + C = G@C \qquad (3)$$

where G is the guest (H_2 or He), C is the host cage (ice cage of the clathrate or the fullerene molecule), and G@C stands for guest encapsulated by the host. At moderate gas pressures P, the equilibrium is fully characterized by the constant K (in atm^{-1}):

$$K = \frac{N[G@C]}{N[G]P} \qquad (4)$$

where N[G@C] and N[C] are number densities of the filled and empty host cages, respectively, and P is the partial pressure of the free guest particles. Assuming spherically symmetrical environment, the equilibrium structure of the system is fully

DOI: 10.1039/b406213b

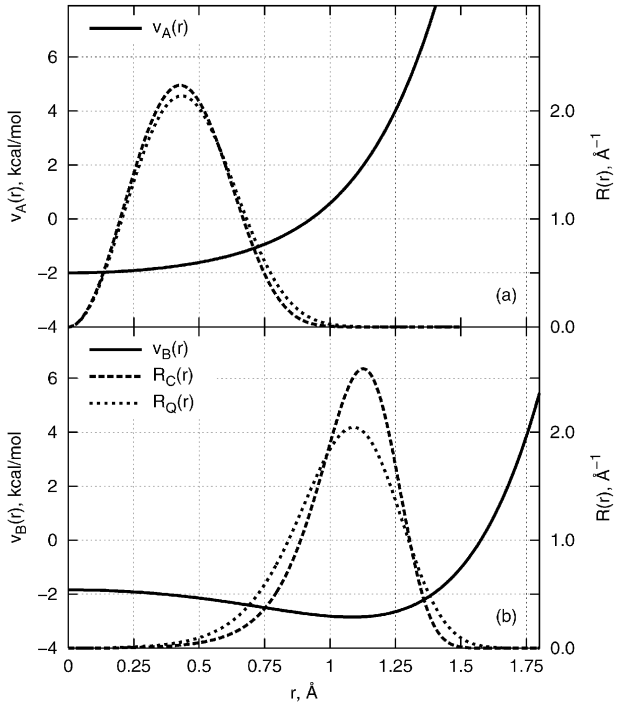

Fig. 1 Interaction potential $v(r)$, classical (R_C) and quantum (R_q) radial distribution functions at 150K. (a) ^{3}He inside buckminsterfullerene C_{60} cage. Classical (quantum) $R_{max} = 0.428$ (0.432) Å, with half-width of 0.439 (0.455) Å. (b) H_2 inside $(H_2O)_{20}$ model clathrate cage. Classical (quantum) $R_{max} = 1.126$ (1.089) Å, with half-width of 0.352 (0.452) Å.

described by the radial distribution function $R(r)$. Both K and $R(r)$ are readily accessible from experiment.

In classical statistics the equilibrium constant is given by:[17,18]

$$K_C = \frac{\lambda^3 Z_C}{kT} \tag{5}$$

where k is Boltzmann constant, T is absolute temperature, $\lambda = h(2\pi mkT)^{-1/2}$ is the "thermal wave length", m is mass of the guest molecule, and h is the Planck constant. Eqn. (5) neglects relaxation of the spherically symmetric host cage. In this approximation, classical partition function Z_C is given by:

$$Z_C = \frac{4\pi}{\lambda^3}\int_0^{r_{max}} \exp\left(-\frac{v(r)}{kT}\right) r^2 dr \tag{6}$$

where r_{max} is cage radius, and $v(r)$ is the guest–host interaction potential. The rigid cage approximation is justified by the separation between frequencies of the guest and host vibrational modes. For a less binding potential such as found for *exohedral* fullerenes, the host vibrations must be taken into account to obtain qualitatively correct results.[6]

Classical radial distribution function for the guest center of mass is given by:

$$R_C(r) = 4\pi V_C^{-1} r^2 \exp\left(-\frac{v(r)}{kT}\right) \tag{7}$$

where the effective volume $V_C = Z_C\lambda^3$. For systems with lower symmetry, standard classical molecular dynamics techniques[8] can be used to calculate K_C and R_C.

In the case of quantum statistics, one particle radial distribution function is given by:

$$R_q(r) = Z_q^{-1} r^2 \sum_i w_i \exp\left(-\frac{\varepsilon_i}{kT}\right) \iint \sin\theta\, |\psi_i(\vec{r})|^2\, d\theta d\phi \tag{8}$$

where ψ_i is one of the eigenfunctions (see below), corresponding to the w_i-degenerate energy level ε_i. The same energy levels determine the canonical partition function Z_q, given by:[18]

$$Z_q = \sum_i w_i \exp\left(-\frac{\varepsilon_i}{kT}\right) \tag{9}$$

The equilibrium constant K_q can be calculated analogous to eqn. (5). Similar to the classical case $V_q = \lambda^3 Z_q$ is the quantum analog of the effective accessible volume V_C. Eigenfunctions and eigenvalues of guest motion are obtained by solving the one particle Schrödinger equation for the motion of the center of mass:

$$\left[-\frac{\hbar^2}{2m}\nabla^2 + v(\vec{r})\right]\psi_i(\vec{r}) = \varepsilon_i\psi_i(\vec{r}) \tag{10}$$

For spherically symmetric potential $v(r)$, this is a standard textbook problem in quantum mechanics. The eigenfunctions of eqn. (10) can be indexed by three quantum numbers k, l, and m:

$$\psi_{klm}(\vec{r}) = Y_{lm}\left(\frac{\vec{r}}{r}\right)\frac{u_{kl}(r)}{r} \tag{11}$$

where Y_{lm} are spherical harmonics and m runs from $-l$ to l. Eigenfunctions with the same primary and orbital quantum numbers k and l are $(2l + 1)$-fold degenerate and share the radial part. The radial functions $u_{kl}(r)$ are solutions of the one-dimensional differential equation:[19]

$$\left[\frac{\hbar^2}{2m}\frac{d^2}{dr^2} + \varepsilon_{kl} - v(\vec{r}) - \frac{\hbar^2 l(l+1)}{2mr^2}\right]u_{kl}(r) = 0 \tag{12}$$

Eqn. (12) is solved subject to the boundary ($u_{kl}(0) = 0$; $u_{kl}(r_{max}) = 0$) and normalization

$$\left(\int_0^{r_{max}} |u_{kl}(r)|^2 dr = 1\right)$$

conditions on the radial wavefunction.

For the potentials v_A and v_B used presently, eqn. (12) has to be solved numerically. We integrate it using Numerov's method,[20,21] on a grid of 1000 equally spaced points distributed between 0 and r_{max}. The eigenvalues are converged to at least 10 significant digits.

Results and discussion

For the helium complex, eqn. (12) is solved for all energy levels up to $E_{max} = 10$ kcal mol^{-1}. This gives 133 energy levels (2191 eigenfunctions), with angular momenta up to $l_{max} = 23$. The ground state is found at -1.53 kcal mol^{-1}, 0.46 kcal mol^{-1} above the potential well bottom. This set of eigenvalues is sufficient for calculating thermodynamic parameters up to $T =$ 900 K ($RT \sim 1.8$ kcal mol^{-1}), the entire temperature range of stability for this species. For the potential v_B (H_2 in $(H_2O)_{20}$ cage), we find 193 energy levels (4009 eigenfunctions) below 10 kcal mol^{-1}. The largest angular momentum is $l_{max} = 30$. The ground state is found at -2.51 kcal mol^{-1}, 0.33 kcal mol^{-1} above the potential well bottom. The bowler hat shape of the potential is reflected in the near-degeneracy of the lowest levels for small angular momenta ($l = 1$: -2.45; $l = 2$: -2.35; $l = 3$: -2.21 kcal mol^{-1}).

For the model A, the interaction potential exhibits a single, non-degenerate minimum at the cage center. As a result, the quantum mechanical and classical radial distribution functions essentially coincide at temperatures above 150 K (Fig. 1). Average structural parameters also show good agreement. For example, at 150 K classical average radial position $\langle r\rangle_C$ is 0.442 Å. The corresponding quantum average $\langle r\rangle_q$ is 0.457 Å.

Even this small difference disappears at 298 K ($\langle r\rangle_C = 0.557$ Å, $\langle r\rangle_q = 0.560$ Å). The distribution half-widths ($r_{1/2}$) agree to 0.02 Å at $T > 150$ K. The classical and quantum radial distributions become indistinguishable above room temperature. This result is not unexpected: the interaction potential v_A is approximately quadratic. In this case, the dynamics of the quantum wavepacket, representing the guest molecule, is formally classical,[22] leading to similar quantum and classical radial distributions. Clearly, classical mechanics is adequate for the structural description of this system above 150 K.

For the more intricate potential B, quantum and classical radial distributions are visibly different at 150 K (Fig. 1b). The most probable quantum and classical positions of the H_2 molecule differ by ~3%, while the half-width changes by more than 25% (0.45 Å *vs.* 0.35 Å). The latter effect should be observable in experimental structure refinement. An even more striking quantum contribution is found for the temperature dependence of the average displacement of the H_2 molecule from the center of the cage. In the classical treatment, $\langle r\rangle$ is essentially constant in the temperature range of 50–300 K (see Fig. 2). The corresponding quantum-mechanical quantity increases by about 5% in the same temperature range. Although the differences decrease at higher temperature, quantum effects remain significant for the entire stability range of this compound ($T \sim$ 150–250 K).

The ratios of the calculated quantum and classical mechanics equilibrium constants for the models A and B are shown on Fig. 3. For the ^{3}He incorporation reaction, believed to occur at temperatures ≥ 600 K, quantum corrections to the equilibrium constant at the reaction temperature amount to less than 3%. This is negligible, compared to other sources of error in the theoretical treatment, and to the experimental uncertainties. At room temperature, the difference increases to about 7%, potentially significant for simulations aiming at chemical accuracy. This example clearly conforms to the conventional wisdom, that quantum-mechanical contributions can be neglected for the equilibrium properties in weakly interacting systems.

The second model case is more interesting. Type II hydrogen clathrate has been characterized at temperatures below ambient (150–250 K). Lower guest mass can be expected to magnify the quantum effects as well. Indeed, for $H_2@(H_2O)_{20}$ quantum effects account for a ~12% decrease in the equilibrium constant at 250 K, and even a ~31% change at 150 K. Assuming that the guest gas loss is responsible for the collapse of the clathrate structure,[15] the quantum contribution corresponds to a ~45 K lowering in the clathrate decomposition temperature—significant for any quantitative study of this system.

Although it would have been difficult to measure the decomposition temperature of a "classical" clathrate, similar differences may be expected for heavier hydrogen isotopes. Indeed,

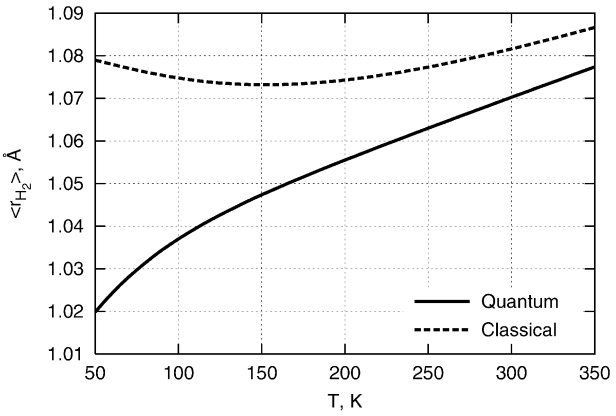

Fig. 2 Temperature dependence of the classical and quantum average radial displacements $\langle r_{H_2}\rangle$ for $H_2@(H_2O)_{20}$.

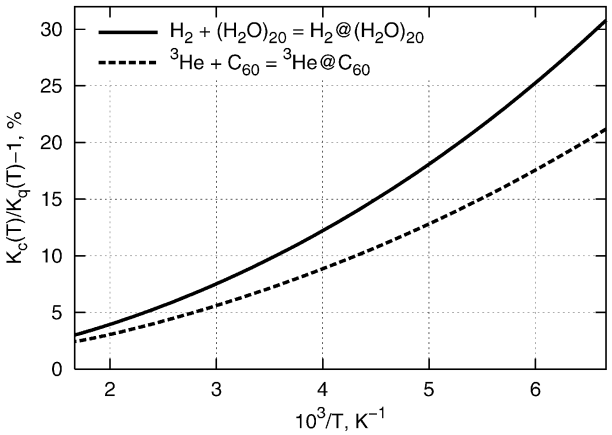

Fig. 3 Ratio of classical and quantum equilibrium constants for the model reactions A ($H_2 + (H_2O)_{20} = H_2@(H_2O)_{20}$) and B ($^3He + C_{60} = {}^3He@C_{60}$), as a function of the inverse temperature.

we calculate quantum-mechanical equilibrium constants of 3.16, 3.44, and 3.60 atm^{-1} for incorporation of respectively H_2, HD, and D_2 at 150 K. This may translate into a ~13 K increase in the decomposition temperature of HD compared to H_2 complex, and ~20 K for D_2 compared to H_2. Thus, formation of clathrate hydrate can provide an efficient fractionation pathway for hydrogen isotopes at sub-zero temperatures and may have significant implications for the models of planetary formation and evolution. Because the structure of type II hydrogen clathrate hydrate contains multiply-occupied cages of different sizes rather than just the singly occupied $(H_2O)_{20}$ cage, these values should be treated as qualitative indications only.

Qualitatively, the relationship between quantum and classical treatments can be revealed by invoking the harmonic oscillator model. In this approximation, classical and quantum partition functions are related by:[23]

$$Z_q = Z_C \prod_i \left(\frac{\beta_i \exp(-\beta_i/2)}{1-\exp(-\beta_i)}\right) \approx Z_C \prod_i \left(1 - \frac{\beta_i^2}{24}\right) \qquad (13)$$

where $\beta_i = h\nu_i/kT$, ν_i being harmonic vibrational frequencies of the system. For small vibrational frequencies ($\beta_i \ll 1$) quantum corrections to the partition function appear only in the second order of β_i. This explains the good qualitative performance of classical simulations at higher temperatures. From eqn. (13), all systems with chemically important motions in the same frequencies range as our model systems (200–400 cm^{-1}) may be expected to exhibit quantum corrections of the same order of magnitude. Because the actual correction factors are sensitive to the shape of particular potential energy surface (compare cases A and B above), quantitative simulations of structure and thermodynamics in such systems would need to consider quantum corrections explicitly. As quantum corrections become more important for anharmonic surfaces, harmonic factors of the eqn. (13) may be insufficient for satisfactory numerical agreement with experiment.

Conclusions

In summary, we demonstrate that quantum effects on molecular motions in weakly interacting systems may become significant at temperatures close to ambient. Strongly anharmonic potentials lead to an increase in quantum corrections. At least in some cases, quantum mechanical terms may contribute tens of percents to calculated equilibrium constants, and to thermally averaged structural parameters. Simulations aiming at achieving chemical accuracy for processes involving soft modes in the 200–400 cm^{-1} range should not blindly neglect quantum effects. Because soft potentials are commonly

encountered in liquid and biomolecular simulations, the importance of quantum-mechanical effects in these systems may need to be reassessed.

We illustrate the influence of the quantum-mechanical effects using the example of the isotope effects in type II hydrogen clathrate hydrate. In this system quantum effects are responsible for a $\sim$14% increase in the calculated equilibrium constants for H_2 incorporation, which may translate to a $\sim$20 K increase in the decomposition temperature of the clathrate at the atmospheric pressure for the fully deuterated compound.

Acknowledgements

The authors thank P. Bunker and J. Tse for stimulating discussions. S. Yu acknowledges financial support from NSERC.

References

1 (*a*) J. S. Tse, *Annu. Rev. Phys. Chem.*, 2002, **53**, 249–290; (*b*) G. D. Billing, *The Quantum Classical Theory*, Oxford University Press, Oxford, 2003.
2 R. J. Hardy, D. J. Lacks and R. C. Shukla, *Phys. Rev. B*, 1998, **57**, 833–838.
3 M. Z. Zgierski and Z. K. Smedarchina, *Europhys. Lett.*, 2003, **63**, 556–561.
4 (*a*) S. Caratzoulas, J. S. Mincer and S. D. Schwartz, *J. Am. Chem. Soc.*, 2002, **124**, 3270–3276; (*b*) Z. Smedarchina, W. Siebrand, A. Fernández-Ramos and Q. Cui, *J. Am. Chem. Soc.*, 2003, **125**, 243–251; (*c*) L. Gorb, Y. Podolyan, J. Leszczynski, W. Siebrand, A. Fernández-Ramos and Z. Smedarchina, *Biopolymers*, 2001, **61**, 77–83; (*d*) S. Bakalova, W. Siebrand, A. Fernández-Ramos, Z. Smedarchina and D. D. Petkov, *J. Phys. Chem. B*, 2002, **106**, 1476–1480.
5 (*a*) J. T. Paci, D. M. Wardlaw and A. D. Bandrauk, *J. Phys. B*, 2003, **36**, 3999–4025; (*b*) E. Perrone, M. D. Poulsen, C. Z. Bisgaard, H. Stapelfeldt and T. Seideman, *Phys. Rev. Lett.*, 2003, **91**, 43003.
6 A. Ruiz, J. Hernández-Rojas, J. Bretón and J. M. G. Llorente, *J. Chem. Phys.*, 2001, **114**, 5156–5163.
7 K. K. Irikura, in *Computational Thermochemistry: Prediction and Estimation of Molecular Thermodynamics (ACS Symposium Series 677)*, ed. K. K. Irikura and D. J. Frurip, American Chemical Society, Washington, DC, 1998.
8 P. Kollman, *Chem. Phys.*, 1993, **93**, 2395–2417.
9 S. Patchkovskii and J. S. Tse, *Proc. Nat. Acad. Sci.*, 2003, **100**, 14645–14650.
10 S. Patchkovskii and W. Thiel, *J. Chem. Phys.*, 1997, **106**, 1796–1799.
11 W. L. Mao, H.-K. Mao, A. F. Goncharov, V. V. Struzhkin, Q. Guo, J. Hu, J. Shu, R. J. Hemley, M. Somayazulu and Y. Zhao, *Science*, 2002, **297**, 2247–2249.
12 T. Weiske, D. K. Böhme, J. Hrušák, W. Krätschmer and H. Schwarz, *H. Angew. Chem. Int. Ed. Engl.*, 1991, **30**, 884–886.
13 M. Saunders, H. A. Jiménez-Vázquez, R. J. Cross, S. Mroczkowski, D. I. Freedberg and F. A. L. Anet, *Nature*, 1994, **367**, 256–258.
14 G. A. Jeffrey, in *Inclusion Compounds*, ed. J. L. Atwood, J. E. D. Davies and D. D. MacNicol, Academic, New York, 1984.
15 J. A. Ripmeester, C. I. Ratcliffe, D. D. Klug and J. S. Tse, *Ann. N. Y. Acad. Sci.*, 1994, **715**, 161–176.
16 (*a*) S. Patchkovskii and W. Thiel, *J. Am. Chem. Soc.*, 1996, **118**, 7164–7172; (*b*) Y. Rubin, T. Jarrosson, G.-W. Wang, M. D. Bartberger, K. N. Houk, G. Schick, M. Saunders and R. J. Cross, *Angew. Chem. Int. Ed.*, 2001, **40**, 1543–1546; (*c*) S. Patchkovskii and W. Thiel, *J. Am. Chem. Soc.*, 1996, **120**, 556–563.
17 H. A. Jiménez-Vázquez and R. J. Cross, *J. Chem. Phys.*, 1996, **104**, 5589–5593.
18 (*a*) T. L. Hill, *An Introduction to Statistical Thermodynamics*, Dover, New York, 1986; (*b*) W. Pauli, *Statistical Mechanics*, Dover, New York, 2000.
19 J. M. Thijssen, *Computational Physics*, Cambridge University Press, Cambridge, 1999.
20 B. Numerov, *Publ. of the Central Astrophys. Observatory. (Rus)*, 1923, **2**, 188–259.
21 The code is available on request.
22 G. D. Billing, *Phys. Chem. Chem. Phys.*, 2002, **4**, 2865–2877.
23 M. Messina, G. K. Schenter and B. C. Garrett, *J. Chem. Phys.*, 1993, **98**, 4120–4127.